



Correlation between platinum–aluminide coating features and tensile behavior of nickel-based superalloy Rene[®]80

Mohammad Mehdi Barjesteh, Seyed Mehdi Abbasi* , Karim Zangeneh Madar, Kourosh Shirvani

Received: 16 September 2018 / Revised: 10 December 2018 / Accepted: 30 April 2019 / Published online: 31 July 2024
© The Nonferrous Metals Society of China and Springer-Verlag GmbH Germany, part of Springer Nature 2019, corrected publication September 2019

Abstract The effect of platinum (a rare metal)–aluminide coating parameters on the tensile properties of nickel-based superalloy Rene[®]80 was evaluated at 871 °C. For this purpose, initial layers of platinum with different thicknesses (2, 4, 6 and 8 μm) were coated on tensile samples. Then, low-temperature high-activity (LTHA) and high-temperature low-activity (HTLA) processes were used for aluminizing. Results of microstructural evaluations using scanning electron microscope (SEM) and phase analysis by X-ray diffraction (XRD) showed a three-layer structure coating for different platinum layer thicknesses and both aluminizing processes. Increasing the thickness of the platinum layer from 2 to 8 μm led to the improvement in the final coating thickness from 91.6 to 102.1 μm in HTLA. This increase was from 128.1 to 148.6 μm in LTHA. The results of hot tensile tests at 871 °C showed a decrease in strength properties of the coated samples compared to the uncoated ones. However, HTLA and high thicknesses of the initial platinum layer showed an intense reduction. The results of fractographic evaluations about uncoated samples showed a ductile fracture. On the other hand, coated samples showed a simultaneous ductile and

brittle fracture failure mechanism. But the main fracture morphology was brittle cleavage fracture which was for the HTLA.

Keywords Rene[®]80; Platinum–aluminide; Aluminizing; Tensile properties; Fractography

1 Introduction

The nickel-based superalloy Rene[®]80, due to its good mechanical properties and corrosion resistance at high temperature, has been widely used in manufacturing turbine blades [1–3]. In most cases, this precipitation-hardened superalloy is generally used at the temperature range of 760–982 °C [4]. In order to enhance its oxidation resistance, aluminide diffusion coatings are used for its surface. At high temperatures, aluminum in the surface of a coated substrate can be oxidized, and a dense alumina layer is formed. This layer acts as a diffusion barrier and reduces the oxidation rate of the substrate [5, 6]. Nowadays, aluminide diffusion coatings (which are based on intermetallic β-NiAl phases) can be modified by rare elements such as platinum to improve their hot corrosion and cyclic oxidation resistance [7–9]. After using the platinum layer, aluminum is diffused into the surface in order to achieve the platinum–aluminide (Pt–aluminide) coatings. It is worthy noting that, based on the aluminum content in aluminizing source, the diffusion treatment can be done by two methods: low-temperature high-activity (LTHA) and high-temperature low-activity (HTLA) [7]. Depending on the thickness of the initial platinum layer and prior diffusion treatment, as well as, aluminizing process, the outer layer of Pt–aluminide coatings may show three main

The original version of this article was revised: In the original publication, Figure 12 was incorrect. Correct Figure 12 has been replaced

M. M. Barjesteh, S. M. Abbasi*, K. Zangeneh Madar
Metallic Materials Research Center, Malek Ashtar University of Technology (MUT), Tehran 158751774, Iran
e-mail: sma_abbasi@mut.ac.ir

K. Shirvani
Department of Advanced Materials and New Energies, Iranian Research Organization for Science and Technology (IROST), Tehran 3313193685, Iran

microstructures which consist of single PtAl₂, dual β -(Ni, Pt)Al + PtAl₂ or single β -(Ni, Pt)Al phase [10]. In the diffusion coatings, the differences in the composition of the coating and substrate, as a result of coating and substrate elements combinations, have a significant effect on the mechanical properties of the alloy.

The study of Rahmani and Nategh [11] showed a declination of yield and ultimate strength properties of Rene[®]80 alloy after applying a plain aluminide coating at 871 °C. Also, Alam et al. [12] evaluated the tensile properties of the CM-247LC alloy with a single-phase Pt–aluminide coating under an LTHA process which showed a different fracture behavior at the temperatures lower and higher than the ductile-to-brittle transition temperature (DBTT). Brittle fracture occurred below DBTT, while ductile fracture was observed above DBTT. They also reported that at the same condition, the DBTT of Pt–aluminide coatings was almost 100 °C higher than that of the plain aluminide coatings. Taylor et al. [13] evaluated the tensile creep properties of a β -rich (Ni, Pt)Al diffusion coating which was used on CMSX4 and Haynes75 under various strains at the temperature range of 800–1000 °C. They found that the tensile creep strength of the diffusion coating was higher than that of the similar coatings tested by the others. They reported that original aluminum and platinum contents of the β -(Ni, Pt)Al coating play a significant role in tensile creep strength of coated alloy. The research conducted by Esin et al. [14] was about the thin-coated alloy AM1 with single-phase Pt–aluminide, indicating that thermal aging led to an increase in coating ductility.

A review about the related studies showed that in spite of some researches on the mechanical properties of the bare Rene[®]80, no evaluation has paid to the effect of Pt–aluminide coating on the mechanical properties, fracture surface and cracking behavior of Rene[®]80 under tensile loading. Also, simultaneous effects of the initial platinum layer thickness and aluminizing methods on tensile properties of superalloy Rene[®]80 have been rarely evaluated.

It should be mentioned that evaluation about the mechanical behavior of Pt–aluminide-coated Rene[®]80 plays a significant role in the design and application of this coating for manufacturing gas turbine engine parts. Therefore, in the present study, the effect of important parameters of Pt–aluminide coating, such as thickness variations of the initial platinum layer (2, 4, 6, 8 μ m) and aluminizing process (HTLA and LTHA), was evaluated on the coating structure and tensile properties of superalloy Rene[®]80 at 871 °C. Also, the variation in tensile properties of superalloy Rene[®]80 with coating parameters was correlated with fracture surface features and cracking behavior of the coatings.

2 Experimental

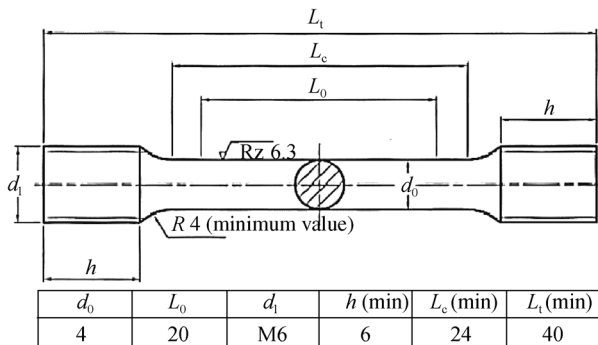
The chemical composition of the nickel-based superalloy Rene[®]80 used as the substrate in this study is listed in Table 1, where Rz, R, d₀, L₀, d₁, h, L_c and L_t are required surface finish, radius, test piece width, original gauge length, width of gripped ends, length of gripped ends, parallel length and total length of test piece, respectively. Before starting the coating process, based on DIN-50125 standard, tensile samples were prepared (according to Fig. 1) through machining of the raw ingots obtained from investment casting. In order to certify the lack of defects in the tensile samples, nondestructive tests such as fluorescent penetration inspection (FPI) and X-ray inspection were carried out according to ASTM E1417 and E1742. The results showed no surficial or internal defects.

The next step involved a solution heat treatment at 1205 °C for 2 h and initial aging treatment at 1095 °C for 4 h. Then, an intermediate nickel layer with a thickness of 1–2 μ m was applied to improve the platinum layer coherence to the surface. Platinum plating was carried out using an electrolyte solution containing 14–18 ml type P salt (Pt (NH₃)₂(NO₂)₂), 70–90 g·L⁻¹ Na₂CO₃, 40–70 g·L⁻¹ NaCH₃COO and 1 L distilled water [15]. Different plating times (3–6 h) (at temperature of 90 °C, current density of 0.2–0.4 A·dm⁻² and pH = 10.5) were used in order to obtain different thicknesses of platinum layer (2, 4, 6 and 8 μ m). Heat treatment of the platinum layer was carried out to increase the adhesion and improve the platinum distribution on the substrate surface at 1050 °C for 2 h. The samples were cooled down to 400 °C in the furnace and then air-cooled [16].

Aluminizing process was carried out using two different methods of LTHA at 750 °C for 4 h followed by post-aluminizing for 2 h at 1050 °C and HTLA at 1050 °C for 2 h using the pack cementation method. The composition of the cementation powder included 2NH₄Cl–12Al–86Al₂O₃ (wt%) and 1NH₄Cl–4Al–95Al₂O₃ (wt%) for LTHA and HTLA methods, respectively. Finally, after the formation of the Pt–aluminide coating on the surface, the samples were aged at 845 °C for 16 h. Before starting the tensile test, microstructural analysis was conducted using a TESCAN scanning electron microscope (SEM) equipped with energy-dispersive spectroscopy (EDS), and in order to ensure the quality of the coating, this analysis was repeated after the test to evaluate the fracture surfaces according to ASTM E3, ASTM E407 and ASTM E883 standards. X-ray diffraction (XRD) analysis was also performed to determine the phase distribution and residual stress of the coatings (Inel Equinox 6000 with X'Pert High Score Plus v2.0, Cu K α 1 with graphite monochromatic, 2 θ = 16°–93°). Microhardness test was carried out perpendicular to the Pt–aluminide coating and its substrate, according to

Table 1 Chemical compositions of nickel-based superalloy Rene[®]80 used in this study (wt%)

C	Cr	Co	Mo	W	Al	Ti	Fe	Zr	V	B	Si	Mn	Ni
0.16	13.81	9.69	4.23	4.02	3.02	4.87	0.12	0.05	0.05	0.02	0.02	0.03	Bal.

**Fig. 1** Dimensions of tensile test sample according to DIN50125 standard (mm)

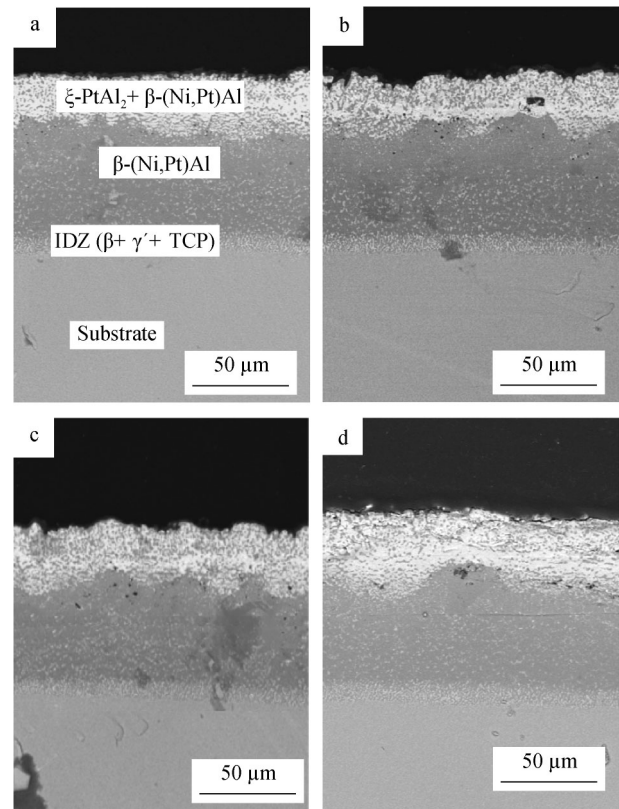
ASTM E384 using an automatic Akashi microhardness set through the application of the force equal to 0.49 N. Macro-hardness measurement was also evaluated based on ASTM E18 using Wilson apparatus under the force of 1471 N on the substrate. Tensile tests were conducted at 871 °C and the strain rate of $1.6 \times 10^{-4} \text{ s}^{-1}$ on the coated and uncoated samples using an ATM CR-100KN machine equipped with an electrical furnace capable of working at temperatures up to 1000 °C, according to the ASTM E21 standard.

3 Results and discussion

3.1 Microstructure of coatings

Before evaluation about the Pt–aluminide coating and after aluminizing process in both methods of LTHA and HTLA, the microstructure and hardness of the substrate were evaluated to test their variability. The results indicated a fixed γ' (Ni₃(Al,Ti)) phase for both LTHA and HTLA methods in a way that the area percentage of this phase was equal to $(38 \pm 4)\%$. Hardness of the alloy was HV 406 and HV 410 for HTLA and LTHA, respectively.

For different platinum thicknesses, the microstructure of the Pt–aluminide was estimated for HTLA and LTHA methods, as shown in Figs. 2, 3, in which, for both aluminizing methods, the microstructure of the outer layer coating included bi-phase encompassing ξ -PtAl₂ and β -(Ni, Pt)Al. The following layers were β -(Ni, Pt)Al (single-phase intermediate layer) and inter-diffusion zone (IDZ, the final layer of coating–substrate interface), respectively. IDZ

**Fig. 2** SEM images of Pt–aluminide coating in HTLA with platinum layer thicknesses of **a** 2 μm, **b** 4 μm, **c** 6 μm and **d** 8 μm

contained β , γ' and topologically closed pack (TCP) phases [14]. The variations in IDZ composition were associated with the segregation of refractory elements such as: tungsten, titanium, chromium, molybdenum and cobalt.

XRD analysis was performed in order to recognize the phases in the coating, especially in ξ -PtAl₂, and ensure the transition of the hard phase of Ni₂Al₃ to the softer phase of β -NiAl in LTHA, and its results are provided in Fig. 4. Accordingly, the PtAl₂ and NiAl phases were identified, which are in good agreement with the results obtained by Krishna et al. [17]. Results also showed the lowest formation of PtAl₂ phase for HTLA with an initial platinum layer thickness of 2 μm, while the highest amount of the PtAl₂ phase was formed in LTHA with a platinum thickness of 8 μm.

Thickness measurement in HTLA and LTHA methods showed a direct effect of platinum layer and aluminizing method on the final thickness of the coatings. Increasing

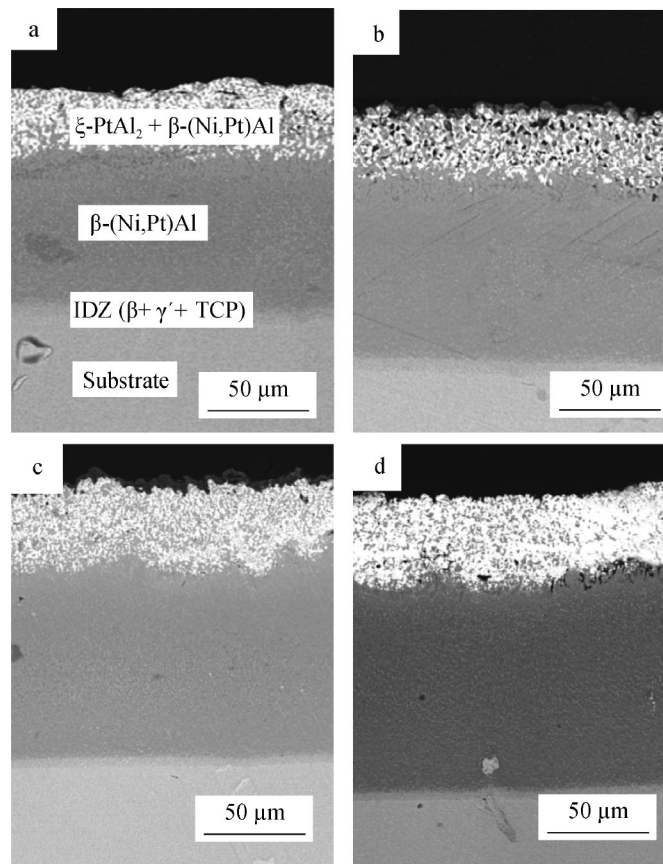


Fig. 3 SEM images of Pt–aluminide coating in LTHA for platinum layer thicknesses of **a** 2 μm , **b** 4 μm , **c** 6 μm and **d** 8 μm

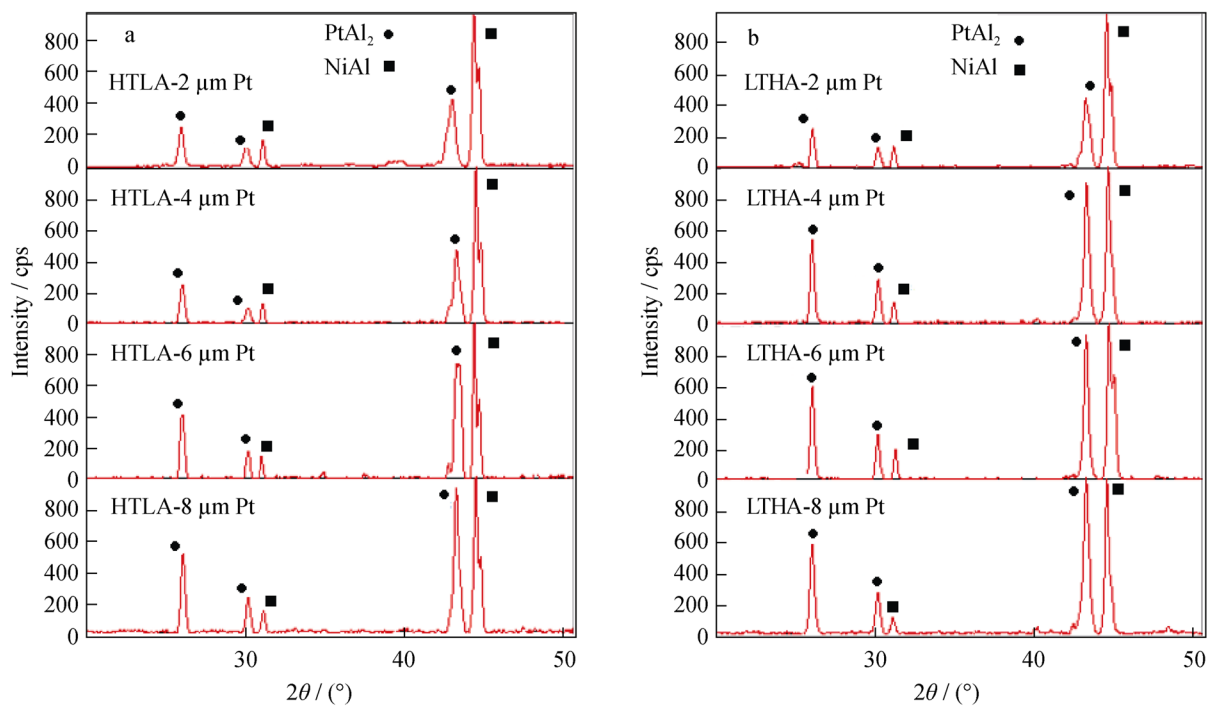


Fig. 4 XRD patterns of samples prepared by **a** HTLA and **b** LTHA methods with different thicknesses of initial platinum layer

the initial platinum layer thickness from 2 to 4, 6 and 8 μm in HTLA method led to final thicknesses of 91.5, 93.5, 95.6 and 102.1 μm , respectively; with the same order, the thicknesses were equal to 128.1, 138.9, 140.4 and 148.6 μm for LTHA method. The variations in the thickness of the Pt–aluminide coating for different initial platinum thicknesses in HTLA and LTHA methods are provided in Table 2 (two sections were measured, and the average value was reported).

Table 2 Thickness of Pt–aluminide layers as a function of initial platinum layer thickness for two aluminizing methods: HTLA and LTHA

Initial thickness/ μm	Phase	Thickness of Pt–aluminide layers/ μm	
		HTLA	LTHA
2	IDZ	8.9	4.5
	β	50.9	84.5
	$\beta + \xi$	31.7	39.1
4	IDZ	9.1	4.9
	β	48.5	93.3
	$\beta + \xi$	35.9	40.7
6	IDZ	10.8	4.3
	β	43.6	92.4
	$\beta + \xi$	41.3	43.7
8	IDZ	13.5	4.4
	β	45.0	97.2
	$\beta + \xi$	43.6	45.4

It can be observed that the increase in initial platinum layer thickness resulted in the enhancement of the β (NiAl) + ξ (PtAl₂) outer layer for both HTLA and LTHA methods, which could be due to the direct relationship between increased initial platinum layer thickness and elevated ξ -PtAl₂ phase content (Fig. 4) [18]. On the other hand, Ni atom diffuses faster in the Pt–containing NiAl structures [19, 20]. Therefore, more Ni atoms can diffuse from substrate to react with Al which will lead to the formation of thicker β -(Ni, Pt)Al coating on the surface. Regarding high amounts of aluminum in LTHA, the thickness of β -(Ni, Pt)Al was also higher than that in HTLA [21]. As a result, relatively thicker ξ -PtAl₂ + β -(Ni, Pt)Al coatings were formed on the samples with thicker platinum plating and higher amount of Al in the aluminizing source. The thickness of the IDZ layer which is the place for the accumulation of refractory elements is also reported to be lower in LTHA in comparison with HTLA. Chromium is an important element of IDZ, which can produce TCP phases (such as σ -(Co, Cr) intermetallic) [22]. As shown in Fig. 5, the distribution of this element was evaluated by EDS line-scan analysis at magnification for both aluminizing methods. Clearly, the presence of chromium in IDZ layer was higher in HTLA method. Indeed, due to the higher thickness of the β layer in LTHA, more chromium content was dissolved in this layer, which resulted in less Cr content of IDZ [18].

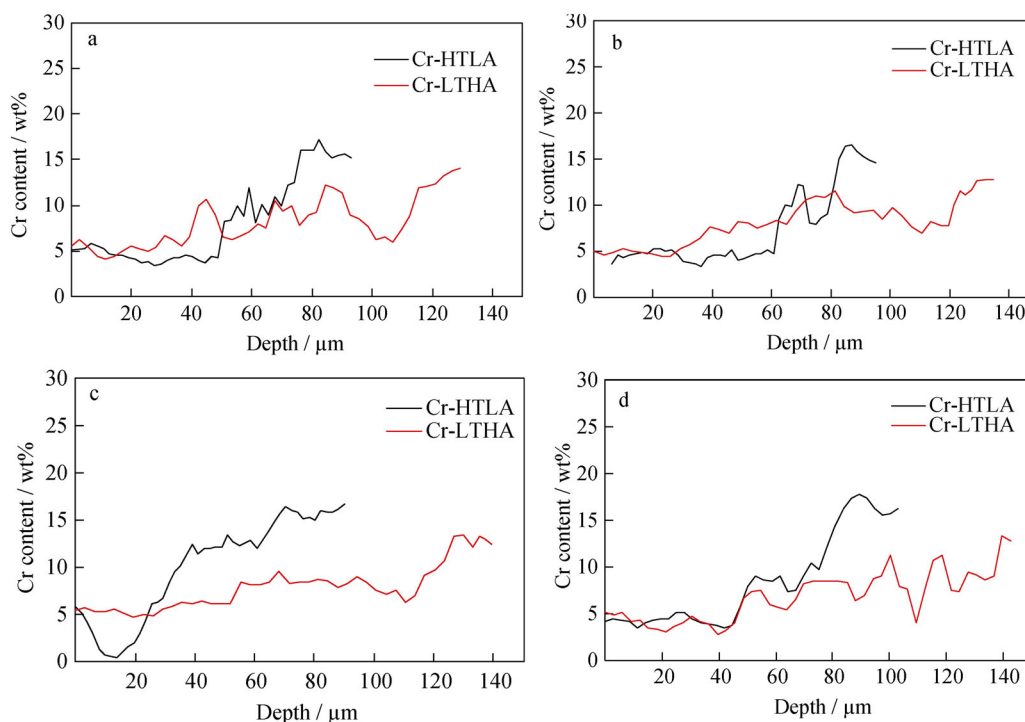


Fig. 5 Comparison of variation of chromium in LTHA and HTLA for platinum layer thicknesses of **a** 2 μm , **b** 4 μm , **c** 6 μm and **d** 8 μm

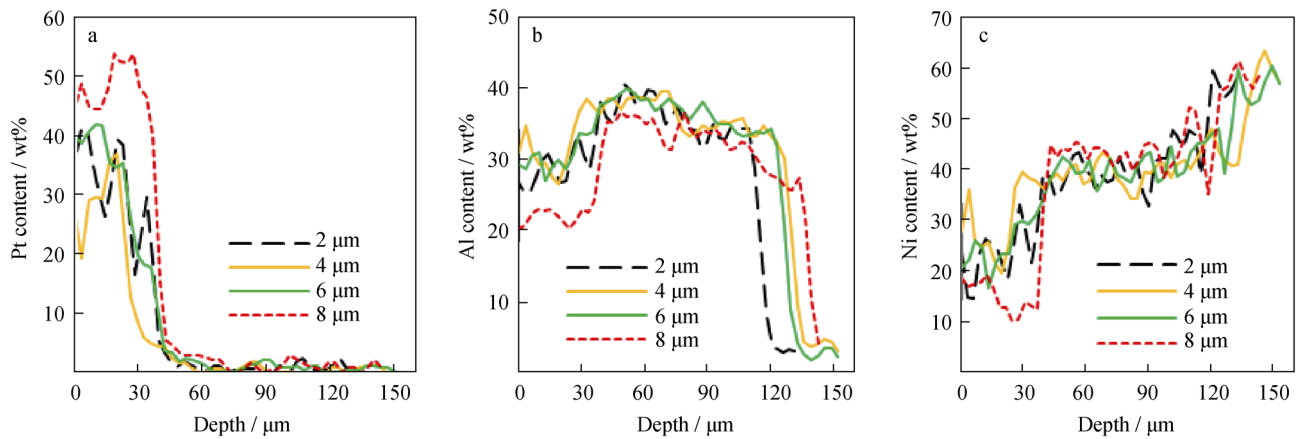


Fig. 6 Variations of concentration and diffusion depth of **a** platinum, **b** aluminum and **c** nickel in LTHA for different platinum layer thicknesses

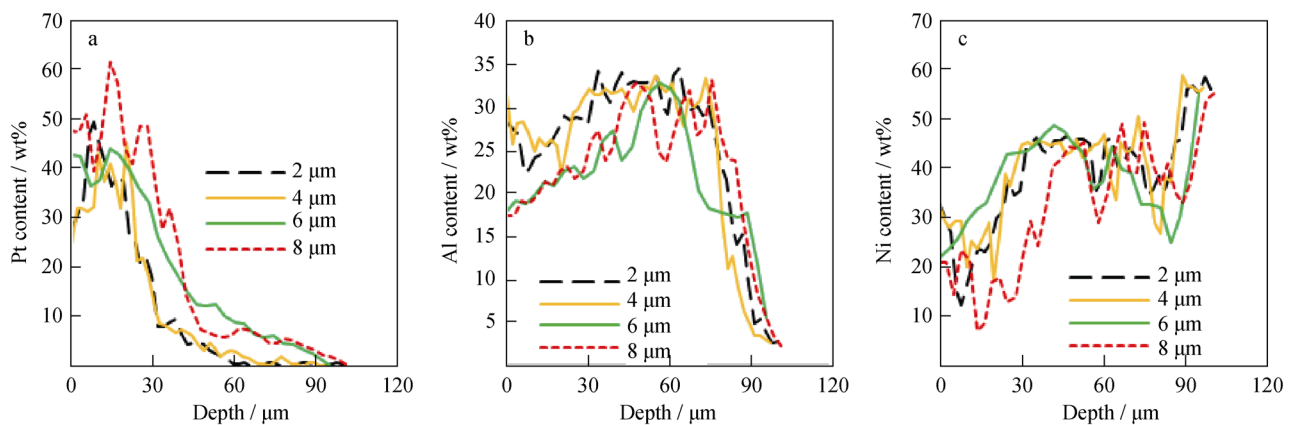


Fig. 7 Variations of concentration and diffusion depth of **a** platinum, **b** aluminum and **c** nickel in HTLA for different platinum layer thicknesses

Figures 6, 7 show the variations of nickel, platinum and aluminum contents in the perpendicular direction of the coatings at different thicknesses of the platinum layer under the two aluminizing conditions (HTLA and LTHA). The results showed an internal diffusion of platinum and aluminum and external diffusion of nickel. Platinum initial thickness also influenced the diffusion depth and concentration gradient of this element.

3.2 Tensile properties

The results of tensile test at 871 °C about the uncoated (after heat treatment according to AMS5403) and coated samples (two samples for each method) are presented in Tables 3 and 4, respectively.

For both LTHA and HTLA methods, yield strength (YS) and ultimate strength (UTS) decreased in coated samples as compared to their uncoated counterparts. The decrease in these properties was bigger in HTLA than in LTHA, which was enhanced by increasing the thickness of the platinum layer. Moreover, compared to those of the uncoated

Table 3 Tensile test results on alloy Rene[®]80 (uncoated) at 871 °C

Samples	UTS/MPa	YS/MPa	EL/%	RA/%
AMS 5403/min	620	415	–	15.0
Sample 1	706	595	9	16.5
Sample 2	696	585	7	15.5

samples, ductility (elongation (EL) and reduction in area (RA)) showed a lower decrease for coated samples with platinum layer thicknesses of 2, 4 and 6 μm in LTHA method. However, in a platinum thickness of 8 μm, this decrease was more intense in LTHA method.

The decrease in tensile properties of coated alloy Rene[®]80 samples can be attributed to the variations in their DBTT. DBTT highly depends on coating process, the coating thickness and chemical composition, phase distribution and microstructure [23]. Below DBTT, the properties of the coating are highly different from the substrate, whereas differences in the properties of the metal coatings and the substrate decrease the temperature range above DBTT [11].

Table 4 Tensile test results on alloy Rene[®]80 coated with different thicknesses of platinum for two aluminizing methods at 871 °C

Aluminizing method	Tensile properties	2 μm		4 μm		6 μm		8 μm	
		Sample 1	Sample 2	Sample 1	Sample 2	Sample 1	Sample 2	Sample 1	Sample 2
HTLA	UTS/MPa	672	658	635	631	558	546	504	492
	YS/MPa	569	561	562	556	525	515	472	462
	EL/%	6.0	6.0	6.5	5.5	6.0	6.0	5.0	4.5
	RA/%	12.5	11.5	12.0	12.0	12.0	12.0	10.5	9.5
LTHA	UTS/MPa	677	663	660	662	655	651	614	602
	YS/MPa	583	573	568	570	550	548	541	531
	EL/%	7.5	7.5	7.0	7.0	7.0	7.0	6.5	6.5
	RA/%	16.0	15.0	15.5	15.5	16.0	16.0	14.5	13.5

Therefore, the working temperature of alloy Rene[®]80 should be chosen in a way that the properties of its coating remain in the ductile range [24]. Alam et al. [25] evaluated DBTT of Pt–aluminide for different platinum layer thicknesses in LTHA. The results of this study showed that by increasing the initial platinum layer thickness, DBTT increased in the sequence of 721, 752 and 795 °C for platinum layer thicknesses of 2, 5 and 10 μm, respectively. Equation (1) shows the direct relationship between enhancements of DBTT and platinum layer thickness [25]:

$$T_{\text{DBTT}} = 698 + 10t_{\text{Pt}} \quad (1)$$

where T_{DBTT} is ductile-to-brittle temperature (°C) and t_{Pt} shows the platinum layer thickness.

In aluminide diffusion coatings, increasing the content of alloy elements in the phase composition (Ni, Pt)Al could lead to an increase in the DBTT range. Moreover, creation of PtAl₂ phase in the outer layer and increase in its amount by platinum content enhancement will finally result in the promotion of this temperature range [25].

Owing to the presence of brittle and intermetallic phases of PtAl₂ and (Ni, Pt)Al in Pt–aluminide coatings, the fracture stress of the coating is lower than that of the substrate. For instance, yield and ultimate strengths of high-activity Pt–aluminide coatings were equal to 200 and 300 MPa at a temperature range of 800–900 °C, respectively [26] which was lower than the yield strength (590 MPa) and ultimate strength (701 MPa) of Rene[®]80 alloy (Table 3). Different fracture stress will be made with this huge difference between the coating and substrate strengths that give rise to the formation of some cracks on the coating during the usage of tensile load. By propagation of these cracks into the substrate, the remained cross section will tolerate lower load. Therefore, these surficial cracks in the coating can explain the reduction in strength properties of coated Rene[®]80 alloy in comparison with those of its uncoated counterpart [12, 24].

It should be mentioned that one of the other causes of decline in strength properties of the alloy was the increase in coating thickness. The cracks which had been formed in high-thickness coatings had higher length and depth, and therefore, higher stress fields will be presented at the crack tip. In the present study, an increase in coating thickness resulted in the decrease in tensile properties for both aluminizing methods (HTLA and LTHA). However, despite higher thickness in LTHA method, the tensile properties showed less decrease compared to those in HTLA, which could be due to other factors such as coating stoichiometric composition and elemental distribution in the coating and substrate, as well as, residual stress which will be addressed next.

Despite bi-phase coatings in HTLA and LTHA methods, the chemical composition and stoichiometry of phases were different due to the differences in aluminum, platinum, nickel and refractory element's content. The single-phase intermediate layer of β-(Ni, Pt)Al played an important role in strength properties of the coatings as it had an effect on DBTT as well as the fracture type [12, 26]. In a perfect stoichiometric state, the atomic ratio of (Ni + Pt):Al is 50:50. In case of any deviation from the perfect stoichiometry (δ), the ratio of (Ni + Pt):Al will be changed to $(50 + \delta)/(50 - \delta)$ [12]. If this deviation (δ) is negative, this phase will be hyper-stoichiometric (Al-rich); otherwise, it is hypo-stoichiometric (Ni-rich), while zero deviation shows a perfect stoichiometry. The effective factors in strength properties are chemical composition of the coatings and their consequent defects in the coatings structure. Vacancy defects are more evident in hyper-stoichiometric coatings, while the substitutional or anti-site defects are dominant prominent in hypo-stoichiometric coatings. In comparison with substitution defects, vacancy defects will result in a higher increase in hardness [27]. In this study, according to Fig. 8, microhardness values of LTHA were higher than those of HTLA. Therefore, it can

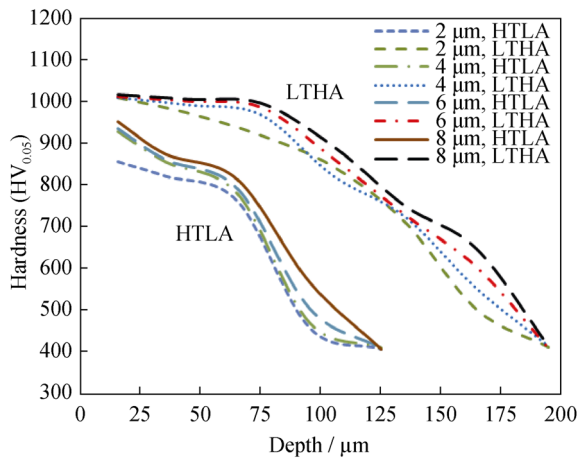


Fig. 8 Variation of microhardness from surface to depth of coating for two aluminizing methods of HTLA and LTHA with different platinum layer thicknesses

be claimed that for a given content of nickel and platinum, due to the high content of aluminum (Figs. 6, 7) in LTHA method, this phase was hyper-stoichiometric in a wide extent of coating thickness. However, in HTLA method, this phase was hypo-stoichiometric. It has been reported that (Ni, Pt)Al phase was more accumulated around the vacancy defects in comparison with substitutional ones [12]. In addition, elastic distortions around these defects can cause a strain field which may further obstruct the dislocation motions. Coating strength in LTHA will be increased by these factors.

Diffusion from the coating to the substrate and vice versa combined with the formation of intermetallic phases are the other effective factors on the reduction in tensile properties. Some of these phases are undesirable and particularly formed in the IDZ. Based on Figs. 2, 3, the IDZ layer thickness was lower in LTHA. Comparison of Cr content in the coatings (according to Fig. 5) showed that Cr content was higher in the coating composition (IDZ) in HTLA method, which could be the result of deleterious phases formation and hence, the reduction in strength properties [22].

Moreover, in LTHA, this is aluminum that diffused in the substrate (inward diffusion), while in HTLA, nickel diffused from substrate to coating (outward diffusion) and the substrate may be depleted from nickel. Nickel is one of the main elements of γ' which strengthens Rene[®]80. In this regard, γ' phase depletion in vicinity of outer surface will be accompanied by a reduction in substrate strength in HTLA method.

More decrease in tensile strength in HTLA could be also assigned to residual stress induced by thermal expansion and elasticity of modulus inconsistency between the

coating and the alloy [28]. XRD analysis was employed to evaluate the residual stress in samples prepared by HTLA and LTHA methods with an initial platinum layer thickness of 8 μm . It must be mentioned that XRD peaks were analyzed using Rietveld analysis in which crystal properties and atomic positions are the essential inputs for simulation of ideal diffraction. Regarding the crystal properties of the present phases, elastic strain of LTHA and HTLA samples were obtained as 1.3×10^{-3} and 2.01×10^{-3} , respectively (by means of X'pert highscore plus software and use of stress-less sample of Y_2O_3). By consideration of the elasticity modulus as 110 GPa [12] and application of Hook's Law [29] the residual stress was calculated as 159.6 and 221.1 MPa for LTHA and HTLA methods, respectively. As it can be seen, the thermal residual stress was higher in HTLA; which could be another reason for higher decline in tensile properties of the mentioned method. Watanabe et al. [30] calculated the residual stress to be 140 MPa for a single-phase Pt–aluminide coating. Moreover, Greving et al. [31] showed that increasing the coating thickness will lead to an enhancement of residual stress. In the present study, promotion of tensile residual stress under the influence of increased coating thickness resulted in higher decline of tensile properties for both HTLA and LTHA methods.

3.3 Fractography

SEM was used for evaluation of fracture surface of the tensile samples for both coated and uncoated samples. Figure 9 shows the fracture surface of an uncoated sample, in which dimples (ductile fracture) could be clearly observed. These dimples included carbide phases, showing that fractures were initiated due to rupture of the carbide-gamma interface. Based on relevant researches [11, 13], fracture phenomenon started from joining of these voids at high temperatures and will finally result in the formation of cracks at grain boundaries and grow along them.

SEM images of the fracture surface in coated samples along the longitudinal direction are provided in Fig. 10. Evaluation about the fracture morphology showed that in LTHA method, fracture surface was similar in all platinum layer thicknesses. Micro-voids can be clearly seen in cleavage fracture within the outer layer and IDZ. The presence of these micro-voids showed ductile fracture and the fact that test temperature was near to DBTT [26]. Fracture morphology of HTLA-prepared specimens was also similar in all platinum layer thicknesses, and micro-voids (ductile fracture) were observable along with cleavage fracture (brittle fracture). However, in comparison with LTHA method, the morphology of cleavage fracture was different, and it could be seen in larger area. This morphology was formed in intermediate and IDZ

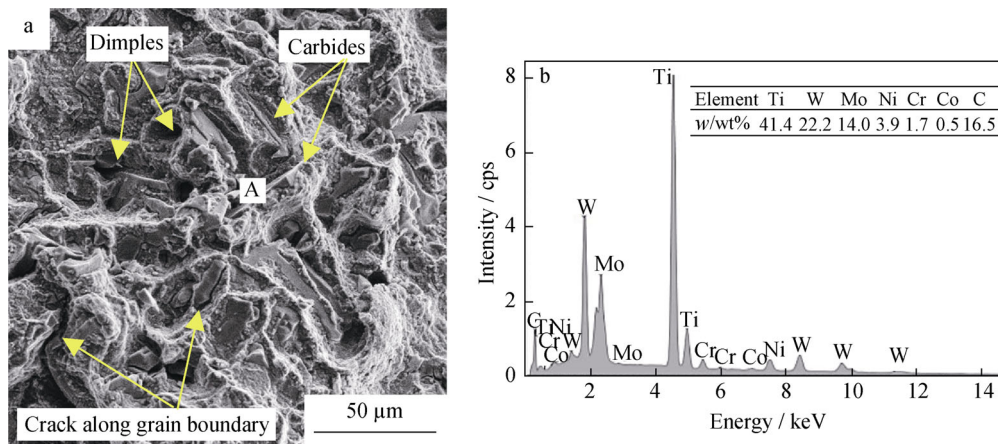


Fig. 9 **a** SEM image of fracture surface of uncoated sample and **b** EDS analysis of Point A

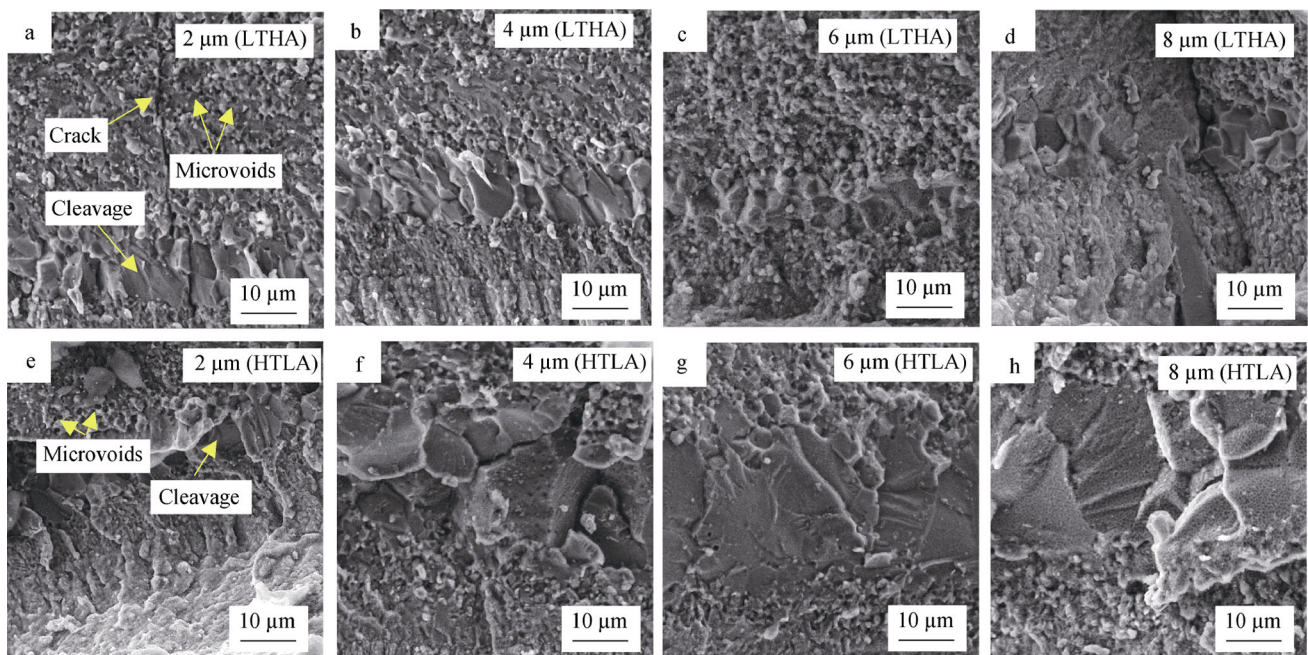


Fig. 10 SEM images of fracture surface of coated samples with platinum layer thicknesses of **a** 2 μm , **b** 4 μm , **c** 6 μm and **d** 8 μm in LTHA and **e** 2 μm , **f** 4 μm , **g** 6 μm and **h** 8 μm in HTLA

layers of HTLA-prepared samples, which was in line with their ductility reduction. As mentioned before, the thickness of the IDZ layer was higher in this state, and a higher percentage of refractory elements could be found in this region, which in turn will give an increase to the formation of deleterious intermetallic phases. Moreover, it was observed that the increase in platinum layer thickness led to the decline of micro-voids concentration and subsequently increased the area of cleavage fracture in both aluminizing methods. These observations were suggested the DBTT enhancement, which agreed with Eq. (1). Therefore, it could be said that the fracture mechanism

was a mixed mode of ductile and brittle fracture for both aluminizing methods and all platinum layer thicknesses. But, as it has been compared to that in LTHA, the extent of brittle fracture was far higher in HTLA. Morphological evaluation about the substrate fracture surface showed similar results for all the coated samples and no difference was found in their fracture morphology when compared with the uncoated samples (Fig. 9). Evaluation about the single-phase β -(Ni, Pt)Al region in both HTLA and LTHA for all platinum layer thicknesses after the test showed that distribution of fine precipitates in this phase was more desirable in LTHA and the particles possessed

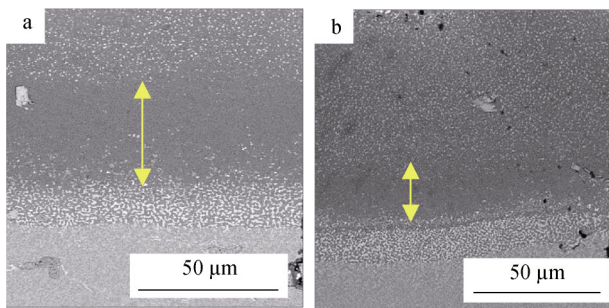


Fig. 11 SEM images of precipitates distribution in β -(Ni, Pt)Al phase in **a** HTLA and **b** LTHA

more uniform dispersion compared to those in HTLA (for example, for the platinum thickness of 6 μm , as provided in Fig. 11). This could be one of the causes of wider cleavage fracture cross section in HTLA. One of the reasons for higher strength of LTHA could be found in this phenomenon, as the presence of these precipitates can inhibit the dislocation movement and thus increase the strength of the coating.

For more precise evaluation about the cracks formed at the surface of coated and uncoated samples, all the samples were cut along longitudinal direction and evaluated by SEM, as shown in Fig. 12a–f. According to Fig. 12a, b, some voids could be observed near the fracture surface of the uncoated samples. These voids were formed through separation of the carbide precipitates from matrix interface. Owing to release of residual stress (from samples machining process) on the surface or near that, some edge cracks were also formed or grown along the grain boundaries of grains recrystallized during aging treatment. Moreover, as the tensile test was conducted at a high temperature (871 $^{\circ}\text{C}$), the brittle oxide layer on the surface could cooperate in the formation and growth of edge cracks. According to Fig. 12c–f, growth of surface cracks for LTHA-prepared sample with a platinum layer thickness of 2 μm (similar to thicknesses of 4 and 6 μm) remained in the coatings range. However, for platinum layer thickness of 8 μm , cracks crossed the IDZ and entered the substrate. In HTLA method, for all the platinum initial layer thicknesses (2, 4, 6 and 8 μm), cracks passed the IDZ and completely diffused into the substrate. In both methods, the increase in final coating thickness increased the thickness and number of cracks, although the number of cracks was higher in HTLA. As diffusion coatings were a part of the substrate, the coating cracks acted as micro-notches in the substrate. By increasing the thickness and number of cracks, the cross section of load bearing will be smaller, and hence the yield and ultimate strength will be declined. This is in complete agreement with the reduction in strength properties of the coated samples, especially for samples prepared by HTLA method.

In Fig. 12g, h, the IDZ was shown at high magnification. Presence of needle-like σ phase [11, 22] was clear in HTLA method (inset in Fig. 12h). Regarding Fig. 5, it could be observed that the chromium content of IDZ was higher in HTLA. However, high chromium content in the IDZ will lead to the formation of σ phase ((Co, Cr) intermetallic) [22] and reduce the ductility (EDS results of the region shown in the inset of Fig. 12h: 15.6 wt% Cr, 9.4 wt% Co, 6.3 wt% Mo, 6.5 wt% W, 6.0 wt% Ti, 52.0 wt% Ni, 4.4 wt% Al). However, due to higher thickness of β -(Ni, Pt)Al phase in samples prepared by LTHA, higher levels of chromium could be dissolved in this region, which may prevent the formation of deleterious phases.

Related researches [17] have reported that Pt–aluminide coatings will improve superalloy resistance to cyclic oxidation and corrosion, when the initial platinum layer thickness was at least 6 μm . As the tensile properties of Rene[®]80 alloy with a platinum layer thickness of 6 μm (prepared by LTHA) did not significantly decrease below the standard tensile characteristics of the uncoated alloy, it could be said that this composition will provide the best resistance for corrosion and cyclic oxidation while preserving the tensile strength. Evidently, by increasing the resistance ability to corrosion and oxidation, the alloy surface will be protected and surface defects could be prevented.

4 Conclusion

In this study, for all platinum layer thicknesses and in both HTLA and LTHA aluminizing methods, ultimate and yield tensile strengths of coated Rene[®]80 decreased at 871 $^{\circ}\text{C}$ in comparison with the uncoated state. However, the increase in platinum layer thickness resulted in a higher decrease in properties, especially in the sample with thickness of 8 μm . These decreases were more intense in HTLA-prepared specimens as compared to LTHA method.

Ductility decreased in both aluminizing methods for all thicknesses of the platinum layer. This decrease was low and approximately fixed up to a platinum layer thickness of 6 μm for LTHA method; however, it became substantial for the platinum layer thickness of 8 μm in both aluminizing methods, which shows that the temperature used for tensile testing was around the DBTT.

For both methods of HTLA and LTHA, the fracture mechanism included a combination of ductile and brittle fracture modes. This further accepted that the test temperature was near DBTT. In comparison with LTHA, the extent of the brittle fracture region was much more in HTLA method.

Micro-cracks were formed in all coatings; for the case of HTLA, they grew into substrate in all the thicknesses,

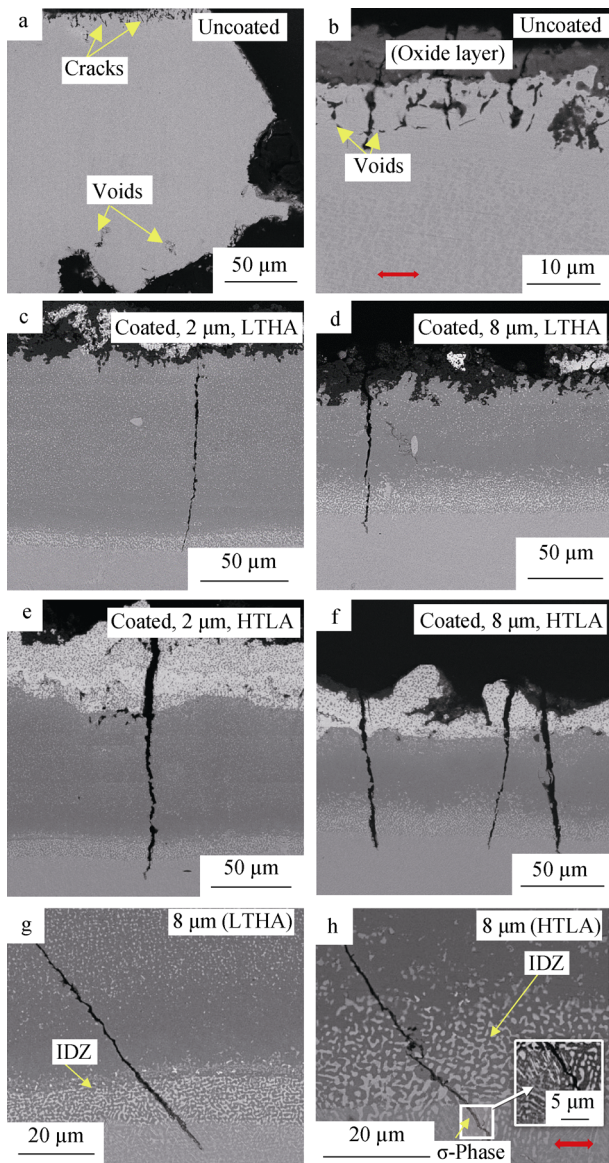


Fig. 12 SEM images of fracture surface (longitudinal section): uncoated tensile samples with **a** fracture end **b** cracks initiated from oxide layer; coated samples with platinum layer thicknesses of **c** 2 μm and **d** 8 μm in LTHA and **e** 2 μm and **f** 8 μm in HTLA methods; IDZ for samples with platinum layer thickness of 8 μm in **g** LTHA and **h** HTLA methods (inset being image of needle-like σ phase)

while in LTHA method, these cracks diffused into substrate only when the sample platinum layer thickness was 8 μm .

References

- [1] Sims CT. A history of superalloy metallurgy for superalloy metallurgists. In: Gell M, editor. *Superalloys 1984*, Champion (USA), 1st ed. Warrendale, PA: The Metallurgical Society. p. 399. https://doi.org/10.7449/1984/Superalloys_1984_399_419.
- [2] Lavella M. Contact properties and wear behaviour of nickel based superalloy René 80. *Metals*. 2016;159(6):1.
- [3] Safari J, Nategh S. On the heat treatment of Rene-80 nickel-base superalloy. *J. Mater. Process. Technol.* 2006;176:240.
- [4] Barjesteh MM, Abbasi SM, Zangeneh Madar K, Shirvani K. The effect of heat treatment on characteristics of the gamma prime phase and hardness of the nickel-based superalloy Rene80. *Mater. Chem. Phys.* 2019;227:46.
- [5] Rafiee H, Arabi H, Rastegari S. Effects of temperature and Al-concentration on formation mechanism of an aluminide coating applied on superalloy IN738LC through a single step low activity gas diffusion process. *J. Alloys Compd.* 2010;505(1):206.
- [6] Zhan Z, Liu Z, Liu J, Li L, Li Z, Pibo L. Microstructure and high-temperature corrosion behaviors of aluminide coatings by low-temperature pack aluminizing process. *Appl. Surf. Sci.* 2010;256(12):3874.
- [7] Streiff R. Protection of materials by advanced high temperature coatings. Primary lecture. *J. Phys. IV*. 1993;3(9):17.
- [8] Shirvani K, Firouzi S, Rashidghamat A. Microstructures and cyclic oxidation behaviour of Pt-free and low-Pt NiAl coatings on the Ni-base superalloy Rene-80. *Corros. Sci.* 2012;55:378.
- [9] Wei LL, Peng H, Zheng L, Sun JY. Processing and oxidation behavior of Pt-diffused coatings. *Rare Met.* 2018. <https://doi.org/10.1007/s12598-017-0982-x>.
- [10] Azarmehr SA, Shirvani K, Schutze M, Galetz M. Microstructural evolution of silicon–platinum modified aluminide coatings on superalloy GTD-111. *Surf. Coat Technol.* 2017;321:455.
- [11] Rahmani K, Nategh S. Influence of aluminide diffusion coating on the tensile properties of the Ni-base superalloy René 80. *Surf. Coat Technol.* 2008;202(8):1385.
- [12] Alam MZ, Kamat SV, Jayaram V, Das DK. Tensile behavior of a free-standing Pt–aluminide (PtAl) bond coat. *Acta Mater.* 2013;61(4):1093.
- [13] Taylor MP, Evans HE, Busso EP, Qian ZQ. Creep properties of a Pt–aluminide coating. *Acta Mater.* 2006;54(12):3241.
- [14] Esin VA, Maurel V, Breton P, Koster A, Selezneff S. Increase in ductility of Pt-modified nickel aluminide coating with high temperature ageing. *Acta Mater.* 2015;105:505.
- [15] Rashidghamat A, Shirvani K. Electrodeposition of platinum on nickel-base superalloy Rene-80. In: *EFC Workshop on Solutions for High Temperature Corrosion Protection in Energy Conversion System*. Frankfurt, Germany. 2009. 24.
- [16] Yavorska M, Sieniawski J. Effect of diffusion on platinum coatings deposited on the surface of nickel based superalloy by the electroplating process. *Arch. Mater. Sci. Eng.* 2010;45(1):56.
- [17] Krishna GR, Das DK, Singh V, Joshi SV. Role of Pt content in the microstructural development and oxidation performance of Pt–aluminide coatings produced using a high-activity aluminizing process. *Mater. Sci. Eng. A*. 1998;251(1–2):40.
- [18] Pedrazaa F, Kennedy AD, Kopecek J, Morettob P. Investigation of the microstructure of platinum-modified aluminide coatings. *Surf. Coat Technol.* 2006;200(12):4032.
- [19] Garg SP, Kale GB, Patil RV, Kundu T. Thermodynamic inter-diffusion coefficient in binary systems with intermediate phases. *Intermetallics*. 1999;7(8):901.
- [20] Kiruthika P, Paul A. A pseudo-binary interdiffusion study in the β -(Ni, Pt)Al phase. *Philos. Mag. Lett.* 2015;95(3):138.
- [21] Das DK, Singh V, Joshi SV. Effect of prealuminizing diffusion treatment on microstructural evolution of high-activity Pt–aluminide coatings. *Metall. Mater. Trans. A*. 2000;31(8):2037.
- [22] Yuan K. Thermal and mechanical behaviors of high temperature coatings. Linköping: Linköping University; 2013. 9.
- [23] Bose S. *High Temperature Coatings*. 1st ed. Oxford: Butterworth–Heinemann; 2007. 123.

- [24] Kolkman HJ. Creep-fatigue and their interaction in coated and uncoated René 80. *Mater. Sci. Eng.* 1987;89:81.
- [25] Alam MZ, Srivathsa B, Kamat SV, Jayaram V, Das DK. Study of Brittle-to-ductile-transition in Pt–aluminide bond coat using micro-tensile testing method. *Trans. Indian Inst. Metals.* 2011; 64(1–2):57.
- [26] Alam MZ, Kamat SV, Jayaram V, Das DK. Micromechanisms of fracture and strengthening in free-standing Pt–aluminide bond coats under tensile loading. *Acta Mater.* 2014;67:278.
- [27] Miracle DB. Physical and mechanical properties of the B2 compound NiAl. *Acta. Metall. Mater.* 1993;41(3):649.
- [28] Tamarin Y. *Protective Coatings for Turbine Blades.* ASM International: Geauga County, Ohio; 2002. 120.
- [29] Newby JR. (Volume Coordinator), *ASM Handbook, Mechanical Testing and Evaluation*, vol. 8. Ohio: ASM International; 2000. 37.
- [30] Watanabe M, Mumm DR, Chiras S, Evans AG. Measurement of the residual stress in a Pt–aluminide bond coat. *Scr. Mater.* 2001;46(1):67.
- [31] Greving DJ, Shadley JR, Rybicki EF. Effects of coating thickness and residual stresses on the bond strength of ASTM C633-79 thermal spray coating test specimens. *J. Thermal. Spray Technol.* 1994;3(4):371.